The EMBO Journal (2007) 26, 720–729 | © 2007 European Molecular Biology Organization | All Rights Reserved 0261-4189/07
www.embojournal.org

THE EMBO JOURNAL

Differential histone modifications mark mouse imprinting control regions during spermatogenesis

Katia Delaval[1], Jérôme Govin[2,3], Frédérique Cerqueira[1,4], Sophie Rousseaux[2,3], Saadi Khochbin[2,3] and Robert Feil[1,*]

[1]Institute of Molecular Genetics, CNRS and University of Montpellier II, Montpellier, France, [2]INSERM, U309, Institut Albert Bonniot, Grenoble, France and [3]Université Joseph Fourier, Grenoble, France

Only some imprinting control regions (ICRs) acquire their DNA methylation in the male germ line. These imprints are protected against the global demethylation of the sperm genome following fertilisation, and are maintained throughout development. We find that in somatic cells and tissues, DNA methylation at these ICRs is associated with histone H4-lysine-20 and H3-lysine-9 trimethylation. The unmethylated allele, in contrast, has H3-lysine-4 dimethylation and H3 acetylation. These differential modifications are also detected at maternally methylated ICRs, and could be involved in the somatic maintenance of imprints. To explore whether the post-fertilisation protection of imprints relates to events during spermatogenesis, we assayed chromatin at stages preceding the global histone-to-protamine exchange. At these stages, H3-lysine-4 methylation and H3 acetylation are enriched at maternally methylated ICRs, but are absent at paternally methylated ICRs. H4 acetylation is enriched at all regions analysed. Thus, paternally and maternally methylated ICRs carry different histone modifications during the stages preceding the global histone-to-protamine exchange. These differences could influence the way ICRs are assembled into specific structures in late spermatogenesis, and may thus influence events after fertilisation.

The EMBO Journal (2007) **26,** 720–729. doi:10.1038/sj.emboj.7601513; Published online 25 January 2007
Subject Categories: chromatin & transcription
Keywords: chromatin; DNA methylation; genomic imprinting; histone methylation; spermatogenesis

Introduction

Genomic imprinting is an essential mechanism in mammalian development whereby certain genes are expressed from one of the two parental alleles only. In the mouse, most imprinted genes are clustered in chromosomal domains, which are broadly conserved in humans. The allelic repression along imprinted domains is mediated by 'imprinting control regions' (ICRs) (Ferguson-Smith and Surani, 2001; Reik and Walter, 2001). These are essential elements of up to several kilobases in size, and most correspond to CpG islands. In somatic cells, the DNA at ICRs is methylated on one of the two parental alleles only. This methylation is inherited from either the female or the male germ line. It provides allele-specific function to the ICR and thus mediates imprinted gene expression (Li *et al*, 1993). At most ICRs, the DNA is methylated on the maternal allele and originates from the female germ line. Only three of the known ICRs are methylated on the paternal allele, and their DNA methylation is established in the male germ line (Delaval and Feil, 2004).

The ICRs with paternal DNA methylation are the one upstream of the *H19* gene at the *H19-Igf2* locus on distal chromosome 7 (the *H19* ICR; Thorvaldsen *et al*, 1998), the ICR upstream of the *Gtl2* gene controlling the *Dlk1-Gtl2* domain on chromosome 12 (the IG-DMR, here referred to as *Gtl2* ICR; Lin *et al*, 2003), and the ICR at the *Rasgrf1* locus on chromosome 9 (the *Rasgrf1* ICR; Yoon *et al*, 2002). At the three ICRs, acquisition of DNA methylation in pro-spermatogonia starts before birth (14.5–18.5 days postcoitum). At the H19 ICR, however, it is fully accomplished in postnatal pachytene spermatocytes only (Davis *et al*, 2000; Ueda *et al*, 2000; Li *et al*, 2004). It is not well understood how DNA methylation is established at the *H19*, *Gtl2* and *Rasgrf1* ICRs, specifically in the male germ line. However, the establishment of methylation at the *H19* and *Gtl2* ICRs involves the DNA methyltransferase Dnmt3a (Kaneda *et al*, 2004), as for the acquisition of methylation imprints in the female germ line (Bourc'his *et al*, 2001).

In contrast to maternally methylated ICRs, the three ICRs with paternal DNA methylation are not known to comprise promoter sequences and are not located within genes either. They do, however, comprise of CpG-rich sequences, as do maternally methylated ICRs (Kobayashi *et al*, 2006). Here, we first explore whether in somatic cells, the maintenance of the differential DNA methylation at the *H19*, *Gtl2* and *Rasgrf1* ICRs is associated with differential chromatin organisation. In particular, we address the question whether specific histone modifications are associated with the DNA-methylated allele at these ICRs, or with the unmethylated allele, and might thus be involved in the somatic maintenance of the differential DNA methylation.

In the mouse, the parental genomes undergo dramatic reductions in DNA methylation after fertilisation, and during pre-implantation development. This is most striking for the sperm-derived genome, which loses most of its DNA methylation following fertilisation of the egg (Mayer *et al*, 2000; Oswald *et al*, 2000). Globally, the genomic DNA in mature sperm is not organised in nucleosomes, but is packaged by

*Corresponding author. Institute of Molecular Genetics, CNRS, UMR5535, 1919 route de Mende, 34293 Montpellier, France.
Tel.: +33 467613663; Fax: +33 467040231;
E-mail: robert.feil@igmm.cnrs.fr
[4]Present address: Institute of Evolutionary Sciences, University of Montpellier II, Montpellier, France

Received: 9 June 2006; accepted: 27 November 2006; published online: 25 January 2007

basic proteins called protamines. The exchange from histones to transition proteins first, and then to protamines, occurs in condensing spermatids during late spermiogenesis (Meistrich *et al*, 2003; Govin *et al*, 2004; Kimmins and Sassone-Corsi, 2005). It is not known whether all DNA sequences undergo this histone-to-protamine exchange and whether this process has an impact on the global DNA demethylation of the paternal genome and on other chromatin changes that occur after fertilisation.

One explanation for the post-fertilisation protection of the *H19*, *Gtl2* and *Rasgrf1* ICRs against the global demethylation would be that this is linked to the establishment of specific structural marks during spermiogenesis, which persist in the male pronucleus when the massive DNA demethylation occurs. As a first step to explore this question, we performed chromatin immunoprecipitation (ChIP) studies at different stages preceding the global histone-to-protamine exchange. In this first locus-specific assay of histone modifications during spermatogenesis, we also included two ICRs with maternally derived methylation: 'region 2' of the *Igf2r* imprinted gene on chromosome 17 (Wutz *et al*, 1997) and the KvDMR1 at the imprinted *Kcnq1* domain on distal chromosome 7 (Fitzpatrick *et al*, 2002). An important insight emerging from these studies is that paternally and maternally methylated ICRs are marked by different combinations of histone modifications at these critical stages preceding histone-to-protamine exchange. We suggest that these differences in histone modifications between the two groups of ICRs, together with their different states of DNA methylation, could impact on their subsequent reorganisation during late spermatogenesis and after fertilisation.

Results

In embryonic cells, the H19, Rasgrf1 and Gtl2 ICRs have allelic H3 methylation and acetylation, and paternal H4 lysine-20 methylation

First, we determined whether ICRs with paternal DNA methylation are marked by allelic histone modifications in somatic cells. ChIP was performed on unfixed undifferentiated embryonic cells and adult tissue. Three ICRs with paternal methylation were analysed. These regions and the extent of their paternal DNA methylation are presented in Figure 1. The ICR controlling the *H19* and *Igf2* genes is located 2–4 kb upstream of the *H19* gene (*H19* ICR) (Thorvaldsen *et al*, 1998). At the *Dlk1-Gtl2* cluster, we analysed the differentially methylated region 10–15 kb upstream of the *Gtl2* gene (*Gtl2* ICR) (Lin *et al*, 2003), which corresponds to a CpG island (Takada *et al*, 2002). The ICR of the *Rasgrf1* locus on chromosome 9 corresponds to a CpG island and is located 30 kb upstream of *Rasgrf1* (*Rasgrf1* ICR) (Yoon *et al*, 2002). As a representative example of an ICR with maternal DNA methylation, we included the KvDMR1. This ICR mediates paternal gene silencing along the *Kcnq1* domain on distal chromosome 7 (Fitzpatrick *et al*, 2002), via a non-coding RNA called *Kcnq1ot1* (Mancini-Dinardo *et al*, 2006).

Unfixed chromatin fragments of 1–7 nucleosomes in length were obtained as described before (Umlauf *et al*, 2004a). After incubation with antisera directed against specific histone modifications, DNA was extracted from the antibody-bound and unbound fractions. Then, using PCR amplification, followed by allelic discrimination applying newly developed single-strand conformation polymorphisms (SSCPs), we determined in each of these fractions the relative abundance of maternal and paternal alleles at the loci of interest. Details about PCR and the oligonucleotides used are provided in Supplementary Table I. The choice of histone H3 and H4 modifications included in the ChIP was based on our previous findings on maternal ICRs (Fournier *et al*, 2002; Umlauf *et al*, 2004a), as well as on studies on constitutive heterochromatin (Peters *et al*, 2003; Martens *et al*, 2005). On histone H3, lysine 9 and 14 acetylation (H3ac), lysine-9 trimethylation (H3K9me3), lysine-4 dimethylation (H3K4me2) and K27 trimethylation (H3K27me3) were analysed. For histone H4, we used an antibody directed against trimethylation on lysine-20 (H4K20me3), a modification that is enriched at pericentric heterochromatin (Martens *et al*, 2005). An antiserum directed against H4 acetylation (at lysines 5, 8, 12 and 16) was also included. Embryonic stem (ES) cells were used as a model to explore early embryonic maintenance. We analysed ES cells of the (C57BL/6 × *Mus spretus*) F1 genotype, thus allowing for SSCP-based discrimination of the parental chromosomes. The ES line studied (SF1-G) was obtained from naturally fertilised blastocysts and it faithfully maintains imprinted expression of *H19*, *Igf2* and *Igf2r* (Dean *et al*, 1998). At the cell culture passages that were used for ChIP (passages 19–21), these cells had unaltered maternal DNA methylation at the KvDMR1, and unaltered paternal DNA methylation at the *H19*, *Rasgrf1* and *Gtl2* ICRs (data not shown).

In agreement with a previous study (Umlauf *et al*, 2004b), H3K4me2 and H3ac were precipitated from the paternal allele predominantly at the KvDMR1. In contrast, the DNA-methylated maternal allele was strongly enriched in the H4K20me3, H3K9me3 and H3K27me3 precipitated fractions (Figure 2A).

Using an SSCP at the 3′-end of the *H19* ICR, we found that the maternal allele was preferentially brought down in

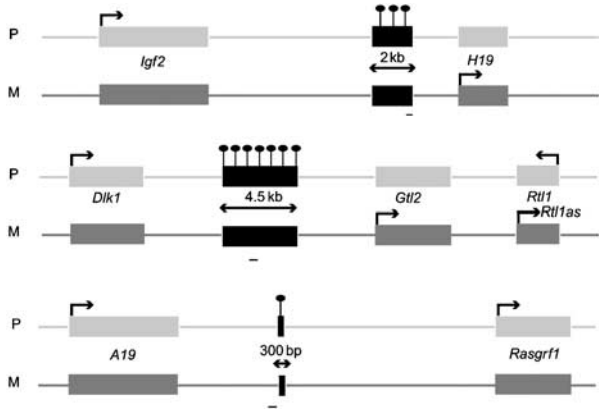

Figure 1 The ICRs of the *Igf2-H19*, *Dlk1-Gtl2* and *Rasgrf1* domains. Genes are represented as grey boxes; arrows indicate their allelic transcription status. ICRs are shown as filled black rectangles; lollipops indicate their paternal CpG methylation. Thin lines indicate regions analysed by PCR amplification and SSCP electrophoresis in precipitated chromatin fractions. The ICR of the *Igf2* and *H19* genes is located 2–4 kb upstream of *H19* (Thorvaldsen *et al*, 1998), and has DNA methylation (indicated as a black bar) on the paternal chromosome (P). The ICR of the *Dlk1-Gtl2* domain is at 10–15 kb upstream of *Gtl2* (Lin *et al*, 2003). Only part of this >1 Mb domain is depicted. Imprinted expression of *Rasgrf1* is controlled by an ICR at 30 kb upstream of the gene (Yoon *et al*, 2002). In the embryo, the paternal methylation covers a region of about 7 kb (Kobayashi *et al*, 2006).

precipitations against H3K4me2 and H3ac. The DNA-methylated paternal allele, in contrast, was strongly enriched in H4K20me3 and H3K9me3 (Figure 2B). No enrichment was observed for H3K27me3 on the DNA-methylated allele.

The allele specificity of the precipitations at the putative *Rasgrf1* ICR was comparable to that of the *H19* ICR. Also here, the unmethylated allele was enriched in precipitations directed against H3K4me2 and H3ac. The DNA-methylated allele, in contrast, was strongly enriched in H3K9me3 and H4K20me3 (Figure 2C). H3K27me3 was not enriched on the DNA-methylated allele, but rather, was precipitated from the unmethylated maternal allele predominantly.

For allelic discrimination at the *Gtl2* ICR, we used an SSCP at the 5′-end of this differentially methylated region (Figure 1). Strong enrichment of H3K4me2 and H3ac was observed on the maternal chromosome. However, in the ES cells, we observed less pronounced allelic enrichment (two-fold) for H4K20me3 and H9K9me3 at this region (Figure 2D). No allelic enrichment of H3K27me3 was observed.

Whereas at all four ICRs, there was a pronounced allelic enrichment in the precipitations with the antiserum directed against H3 K9 + K14 acetylation (H3ac) (and also with an antiserum directed against H3 K9 acetylation only; data not shown), there was no apparent allelic enrichment of H4 acetylation at the *H19*, *Gtl2* and *Rasgrf1* ICRs, and there was only a moderate allelic enrichment at the KvDMR1 (data not shown). Thus, in ES cells, the three ICRs with paternal DNA methylation have specific histone modifications (H3K9me3 and H4K20me3) associated preferentially with the methylated allele, and others (H3K4me2, H3ac) with the unmethylated allele. H3K27me3, however, was not consistently associated with the DNA-methylated allele at all ICRs analysed.

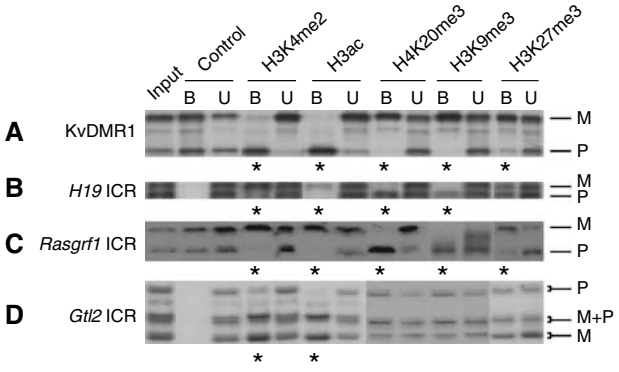

Figure 2 Allelic histone modifications at different ICRs in ES cells. ChIP was performed against H3 lysine-4 dimethylation (H3K4me2), H3 lysine-9 + 14 acetylation (H3ac), H4 lysine-20 trimethylation (H4K20me3), H3 lysine-9 trimethylation (H3K9me3) or H3 lysine-27 trimethylation (H3K27me3). DNA extracted from antibody-bound (B) and unbound (U) fractions was PCR amplified, followed by electrophoretic detection of SSCPs. In each panel, the left lane shows the input chromatin, followed by a control ChIP (C) without a histone-specific antiserum. For each of the bound fractions, we determined the ratio between the maternal (M) and paternal (P) alleles. Asterisks indicate ChIP samples where, after correction against the allelic ratio in the input chromatin, the allelic ratio was higher than 3 (more than three-fold allelic enrichment). Typically, where only one parental allele is visible in the bound fraction, this corresponds to a >15-fold enrichment. (**A**) The KvDMR1 regulates imprinted expression along the *Kcnq1* domain. The analysed region is at 100 bp from the *Kcnq1ot1* transcription start site. (**B**) The *H19* ICR. PCR–SSCP was performed at a region located 2 kb upstream of *H19*. (**C**) The ICR of the *Rasgrf1* domain. A region at 200 bp from this ICR was analysed by PCR–SSCP. (**D**) The ICR of the *Dlk1-Gtl2* domain.

Allelic histone modifications are maintained in adult somatic cells

Next, we determined whether the allelic histone modifications at the *H19*, *Rasgrf1* and *Gtl2* ICRs are maintained in adult tissue cells as well. For this, we performed crosses between C57BL/6 females and males of a *Mus musculus molosinus* inbred strain, to obtain offspring in which all the regions of interest were hybrid between the two subspecies. Adult liver was dissected and used for ChIP. As for the ES cells, maternal and paternal alleles could be distinguished by PCR followed by electrophoretic detection of SSCPs. DNA sequence details and PCR primers are provided in Supplementary Table I. As a control, we first analysed the KvDMR1, which, as in ES cells, had an enrichment of H3K4me2 and H3ac on the unmethylated paternal allele and enrichment of H3K9me3, H4K20me3 and H3K27me3 on the DNA-methylated maternal allele (Figure 3A).

At the *H19* ICR, we detected H3K4me2 and H3ac on the maternal allele, whereas the paternal, DNA-methylated, allele was enriched in H4K20me3 and H3K9me3. As in the ES cells, we observed no allelic enrichment in H3K27me3 (Figure 3B) or H4 acetylation (data not shown).

Similarly, the *Rasgrf1* ICR had maternal H3K4me2 and H3ac, and pronounced paternal H4K20me3 and H3K9me3 in the chromatin obtained from liver (Figure 3C). As in ES cells, there was allelic H3K27me3 enrichment on the maternal allele.

Parental allele-specific precipitation was observed at the *Gtl2* ICR as well, as in ES cells. Here also, the maternal allele was enriched in H3K4me2 and H3ac, whereas the paternal allele was strongly enriched in H4K20me3 and H3K9me3. No allelic enrichment was observed for H3K27me3.

Our data indicate that the allelic histone modifications at the ICRs are comparable in ES cells and adult tissue. Specific histone modifications are consistently associated with the DNA-methylated allele (H4K20me3 and H3K9me3), and others with the unmethylated allele (H3K4me2 and H3ac). H3K27me3, however, is not associated with the DNA-methylated allele at each of the ICRs analysed, neither in ES cells nor in liver.

To determine the relative levels of precipitation at the different ICRs analysed, we performed real-time PCR amplification on the immunoprecipitated chromatin fractions (Figure 3E). For H3K4me2, the highest levels of precipitation were observed at the KvDMR1 and the lowest ones at the *Rasgrf1* ICR. Also for H3ac, the highest levels of precipitation were at the KvDMR1. H4K20me3 and H3K9me3 were precipitated at comparable levels at all the four ICRs. Precipitation levels of H3K27me3 were high at all the regions and highest at the *Rasgrf1* ICR.

In spermatogenic cells, the H19, Gtl2 and Rasgrf1 ICRs have histone modifications different from those of the KvDMR1 and Igf2r ICRs

The *H19, Gtl2* and *Rasgrf1* ICRs are exceptional as their DNA methylation is established during spermatogenesis, at an

early stage before the onset of meiosis. Following fertilisation, this methylation is maintained throughout development, in all the somatic lineages. In early embryonic cells and later in development, the maintenance of DNA methylation could be linked to the presence of specific histone modifications, including the H4K20me3 and H3K9me3 that we detected in ES and adult cells. It is unclear what protects these regions against the global DNA demethylation that occurs after fertilisation (Mayer *et al*, 2000; Oswald *et al*, 2000). This question is difficult to address in mature sperm, given the technical difficulties in extracting and studying DNA-packaging structures in this densely-compacted context (Gatewood *et al*, 1987; Gardiner-Garden *et al*, 1998). As a first step to address this key question, we chose to analyse the stages of spermatogenesis that precede the global histones-to-protamine exchange (Govin *et al*, 2004; Kimmins and Sassone-Corsi, 2005). Our specific aim was to determine whether paternal ICRs are marked by specific histone modifications at these critical stages, and could consequently be recognised differently during the subsequent chromatin remodelling (Figure 4A).

Germ cells were analysed at three spermatogenic stages: spermatocytes, round spermatids (steps 1–8) and elongating spermatids (steps 9–11). Pure fractions of primary spermatocytes and round spermatids were reproducibly obtained from testes from 8-week-old mice. This was carried out by separating cells through BSA gradients according to their size and molecular density, as described before (Bellve, 1993; Pivot-Pajot *et al*, 2003). Using the same approach for purifying elongating spermatids, we routinely obtained a mixture of elongating spermatids (70%) and round spermatids (30%). Condensing spermatids (steps 12–16) were not included in this study, as these have largely initiated the histone-to-protamine exchange and the chromatin is no longer accessible to standard micrococcal nuclease (MNase) fractionation. By Western blotting, we first assessed the overall levels of the different histone modifications. This was carried out in two independent experiments (Figure 4B): spermatocytes

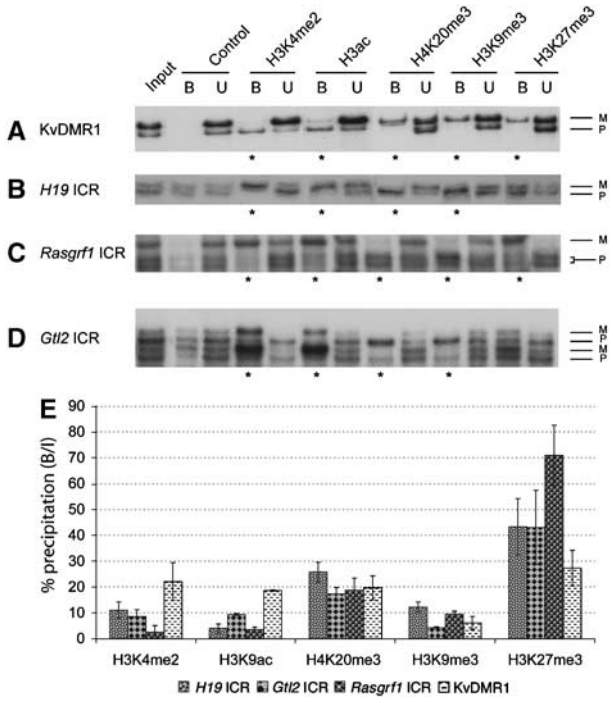

Figure 3 Allele-specific histone methylation and acetylation in liver. ChIP and allelic discrimination by PCR–SSCP were as for ES cells. Asterisks indicate the lanes where, after correction against the allelic ratio in the input chromatin, the allelic ratios were higher than 3. Typically, where only one parental allele is visible in the bound fraction, this corresponds to a >15-fold enrichment. Shown are ChIP data for KvDMR1 (**A**), *H19* ICR (**B**), *Rasgrf1* ICR (**C**) and *Gtl2* ICR (**D**). (**E**) For quantification of histone modifications, ChIP samples were analysed by real-time PCR. Levels of precipitation are shown as the percentage of the input chromatin that was precipitated in the antibody-bound fractions.

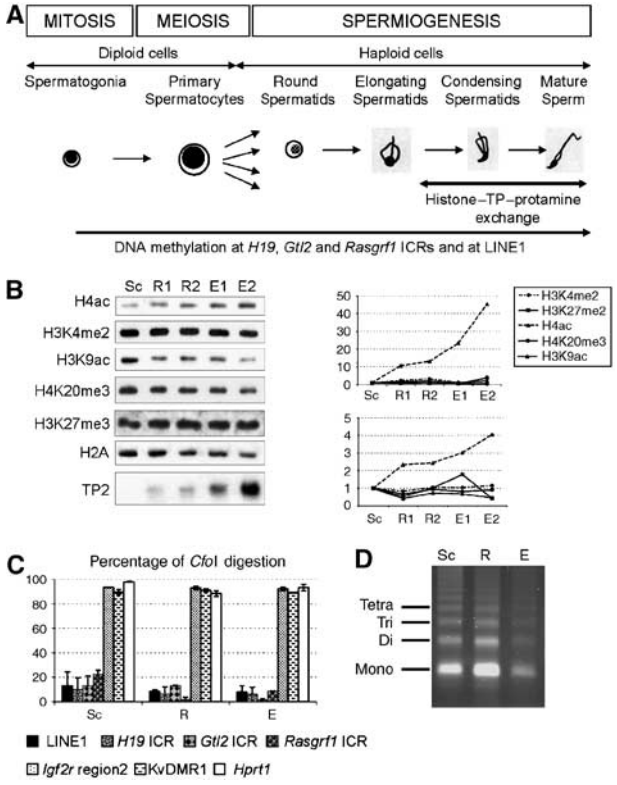

Figure 4 Levels of histone modifications and DNA methylation at different spermatogenic stages. (**A**) Schematic representation of spermatogenesis and the different spermatogenic stages. The line with arrowhead on the right indicates when DNA methylation is detected at the *H19*, *Gtl2* and *Rasgrf1* ICRs and at LINE1 repeats. (**B**) Total protein fractions corresponding to spermatocytes (Sc), round (samples R1 and R2) and elongating spermatids (E1 and E2) were used for Western blotting. Equal amounts of protein were loaded in the different lanes. Immunostaining was with antisera against different histone modifications, histone H2A and transition protein TP2. Measured band intensities were normalised using H2A, and are presented in the graph to the right. The additional graph display presents data from an independent second experiment. Note that the elongating spermatid fraction 2 corresponds to a later stage than fraction 1, explaining the higher TP2 expression. (**C**) Analysis of DNA methylation at ICRs in spermatocytes and round and elongating spermatids. Total genomic DNA was digested with the methylation-sensitive enzyme *Cfo*I, followed by real-time PCR amplification across the ICRs of *H19*, *Rasgrf1*, *Gtl2*, KvDMR1 and *Igf2r* region 2. Also included are the *Hprt1* CpG island and LINE1 sequences. Plotted for each locus is the percentage of DNA digested by *Cfo*I. (**D**) Purification of unfixed chromatin fragments from spermatocytes and round and elongating spermatids. Extracted nuclei were incubated for a short time in a buffer containing MNase. DNA was purified and electrophoresed through a 1% agarose gel, followed by ethidium bromide staining of the gel. In all three preparations, chromatin fragments were 1–7 nucleosomes in length.

(Sc), two successive fractions of round spermatids (R1 and R2) and two fractions of elongating spermatids (E1 and E2, containing about 40 and 25% of round spermatids, respectively). To monitor the developmental transitions between these stages, we included TP2, a transition protein that accumulates in elongating spermatids (Meistrich *et al*, 2003). To demonstrate persistence of nucleosomes at these stages, we included an antiserum directed against core histone H2A. Global levels of H3K9ac, H3K4me2 and H4K20me3 did not vary significantly among the three spermatogenic stages.

We next determined whether the *H19*, *Gtl2* and *Rasgrf1* ICRs were DNA-methylated in the purified spermatocytes, round spermatids and elongating spermatids. Also studied were the KvDMR1 (Fitzpatrick *et al*, 2002) and another maternally methylated ICR, 'region-2' of the *Igf2r* gene (Wutz *et al*, 1997). As an additional control, we included the promoter of the *Hprt1* gene on the X chromosome, a CpG island not involved in imprinting. To also consider DNA-methylated repeat elements and to determine whether these are comparable to methylated ICR elements, we included LINE1 repeats (LINE1). Genomic DNA was extracted from the germ cells corresponding to each of the three spermatogenic stages, and was digested with the methylation-sensitive restriction endonuclease *Cfo*I, which cleaves its recognition sequence (5′-GCGC-3′) only when it is unmethylated. Each of the regions analysed had one or several *Cfo*I restriction sites (see Supplementary Table II). Following digestion, we determined by real-time PCR amplification (for primers, see Supplementary Table II) the percentage of DNA that had been cleaved by *Cfo*I (Figure 4C). This showed that in spermatocytes and in round and elongating spermatids, the *H19*, *Gtl2* and *Rasgrf1* ICRs and LINE1 sequences had high levels of DNA methylation, whereas only low levels of methylation were detected at the KvDMR1, *Igf2r* region 2 and *Hprt1*.

To analyse in detail the histone modifications at the different ICRs, we devised a protocol to obtain unfixed chromatin fragments from spermatocytes, round spermatids and elongating spermatids (Figure 4D; Materials and methods). One characteristic of these germ cells was that their genome was largely accessible to digestion by MNase. Upon short incubation of purified nuclei in a buffer containing MNase, most of the chromatin became digested into fragments of 1–7 nucleosomes in length. These oligonucleosomes were readily retrieved in the soluble chromatin fraction (Figure 4D). Importantly, we verified that none of the regions analysed was retained in the non-fractionated 'pellet' fraction (data not shown). After purification, the germ cell chromatin was precipitated exactly as for ChIP on somatic cells. We focused on the histone modifications that we had found to be allele specific in ES and liver, reasoning that these could be differentially present in germ cells as well. Besides the *H19*, *Gtl2* and *Rasgrf1* ICRs, we included the KvDMR1, the region 2 of *Igf2r*, the *Hprt1* CpG island and LINE1 sequences.

In the antibody-bound fractions, we determined by real-time PCR (see Materials and methods) the percentage of the input chromatin precipitated at the different loci (Figure 5). Histone H4 acetylation was readily precipitated at all the different loci analysed, with 10–40% of the input chromatin brought down in spermatocytes, round and elongating spermatids. Thus, considerable levels of H4 acetylation are present at all the loci analysed, including the ones at which the DNA is fully methylated (*H19*, *Gtl2*, *Rasgrf1*, LINE1). At LINE1 repeats and *Hprt1*, levels of H4ac increased progressively from the spermatocyte to the elongated spermatid stage, following the global trend observed by Western blotting (Figure 4B). At the ICRs, levels of H4ac were comparable at the different spermatogenetic stages analysed.

For H3 K9 acetylation, a rather different result was obtained. H3 acetylation was detected at the KvDMR1, *Igf2r* and *Hprt1* regions, but was absent or strongly reduced at the *H19*, *Gtl2* and *Rasgrf1* ICRs and at LINE1 repeats (Figure 5C). Thus, whereas H4 acetylation was present at all the loci analysed, H3 acetylation was preferentially present at the (promoter) regions that had no DNA methylation at the three spermatogenic stages analysed.

Relative levels of H3K4me2 were similar to those obtained for H3 acetylation. Particularly, in the spermatocytes, round and elongating spermatid fractions, high levels of H3K4me2 were detected at the KvDMR1 and *Igf2r* ICRs, and also at *Hprt1*. In contrast, there was little precipitation at the *H19*, *Gtl2* and *Rasgrf1* ICRs, and at LINE1 sequences, in particular in round and elongating spermatids.

Combined, these data indicate that the *Igf2r* and KvDMR1 ICRs and the *Hprt1* CpG island have H3 lysine-4 methylation and H3 acetylation in spermatocytes and in round and elongating spermatids. The DNA-methylated *H19*, *Gtl2* and *Rasgrf1*, and LINE1 sequences are depleted for these modifications at these critical stages preceding the global histone-to-protamine exchange. We checked that these pronounced differences between the different ICRs were not due to differential presence of histone H3. For this, we included a polyclonal antiserum against histone H3. Similar levels of precipitation were achieved at all the regions analysed, indicating that histones H3 are similarly present at the regions analysed.

Levels of H4K20me3 were low at all the ICRs analysed. Interestingly, however, there were significantly higher levels of H4K20me3 at the LINE1 repeats (Figure 5). We also used an antiserum directed against H3-K9me3, but this did not give quantitative precipitation above background levels at any of the ICR elements analysed (data not shown). H3K27me3 was precipitated at similar levels at all the ICRs analysed, and at LINE1 repeats.

In conclusion, in the male germ cells, the combinations of histone modifications at *H19*, *Gtl2* and *Rasgrf1* are different from those at KvDMR1, *Igf2r* region 2 and *Hprt1*. Another distinction of these regions is that they have DNA methylation, whereas the maternal ICRs are unmethylated in spermatocytes and during the postmeiotic stages of spermatogenesis (Figure 4B). These methylated sequences are unlikely to be expressed as they do not correspond to promoters. Indeed, we did not find the sequences of the *H19*, *Gtl2* and *Rasgrf1* ICRs in databases of expressed sequence tags (ESTs) derived from testis and adult and embryonic tissues. Accordingly, at the regions analysed by ChIP, we also did not achieve any amplification from cDNA (data not shown). The KvDMR1 and the *Hprt1* CpG island, in contrast, are promoters and could, thus, be transcriptionally active in the spermatogenic cells. To explore such a possible link with gene expression, we made cDNA from spermatocytes and round and elongating spermatids, and determined the mRNA levels for *Hprt1* and the KvDMR1 (the *Kcnq1ot1*

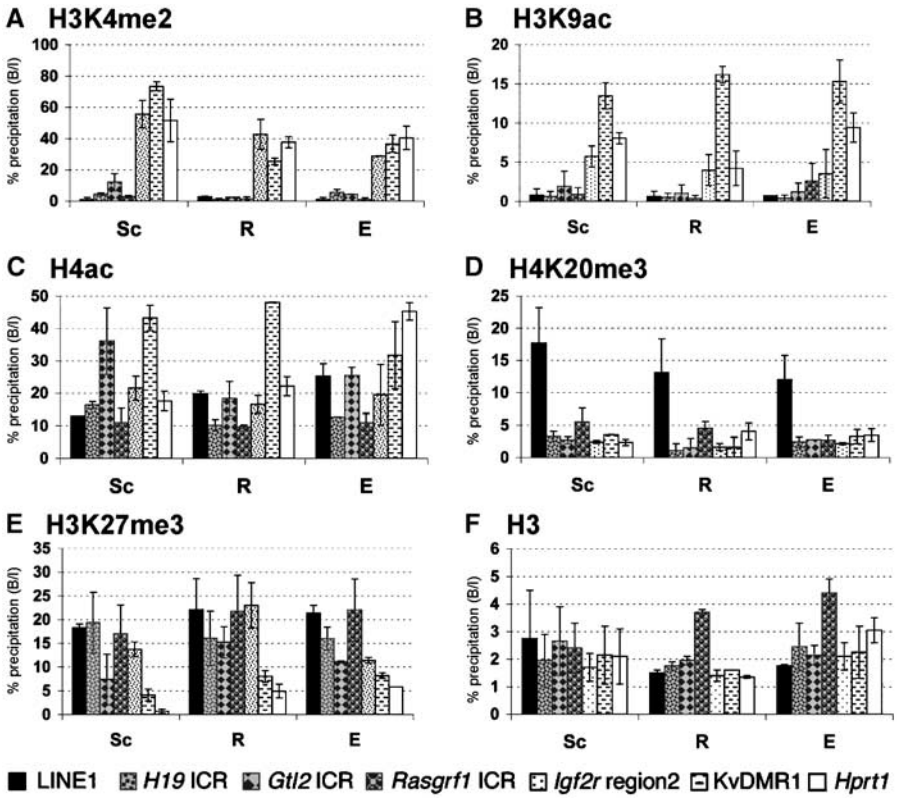

Figure 5 H3 modifications distinguish different ICRs in spermatocytes and at postmeiotic stages of spermatogenesis. Levels of H3K4me2 (**A**), H3K9ac (**B**), H4ac (**C**), H4K20me3 (**D**), H3K27me3 (**E**) and total H3 (**F**) were assessed in spermatocytes (Sc), in round spermatids (R), and in elongating spermatids (E), by ChIP followed by quantitative PCR. For each graph, precipitation is shown as the percentage of input chromatin (I) that was brought down by the specific antiserum (B, for bound fraction) at the locus of interest. Values are the average of two to three independent ChIP experiments, and were corrected for background levels of precipitation at the different loci analysed (background precipitation was determined with a non-histone related antiserum and was $<3\%$ at all regions analysed).

non-coding transcript). Transcripts for both mRNAs were detected at all stages, but expression levels were much lower than those of the B-actin gene. *Tnp1*, a transition protein (Meistrich *et al*, 2003), becomes highly expressed during spermiogenesis (Table I). Our findings confirm a recent study on *Hprt1* showing that this X-linked gene is lowly expressed in spermatocytes and does not become upregulated during spermiogenesis (Namekawa *et al*, 2006). RNA levels of *Dlk1*, a gene reported not to be expressed in the testis, were even lower, and there was no detectable expression of the *Air* transcript (from the *Igf2r* region 2; Seidl *et al*, 2006). Thus, although the KvDMR1, *Igf2r* ICR and the *Hprt*1 CpG island correspond all three to promoter regions, the relative enrichments of their chromatin in H3K4me2 and H3 acetylation at these spermatogenic stages do not correlate with their relative levels of expression at these developmental stages.

Table I mRNA expression in spermatogenic cells and adult tissues[a]

	Hprt1	β-Actin	*Tnp1*	*Dlk1*	*Kcnq1ot1*
Spermatocytes (Sc)	1	298	179	0.05	1.38
round spermatids (R)	1	575	983	0.11	0.88
elongating spermatids (E)	1	970	2918	0.09	1.48
Testis	1	191	77.5	0.07	0.02
Brain	1	70	0.001	0.93	0.05
Liver	1	1.2	—[b]	—[b]	0.02

[a]Expression levels were corrected against *Hprt1* expression, which was defined as 1.
[b]Below detection; expression of the non-coding *Air* transcript was below detection in all samples.

Differential precipitation of H3 lysine 4 methylation in premeiotic germ cells

Our finding in the meiotic (spermatocytes) and postmeiotic (round and elongating spermatids) spermatogenic cells of H3K4me2 and H3 acetylation at the KvDMR1 and *Igf2r* region 2 raises the question whether these modifications are linked to the absence of DNA methylation. These modifications were detected at only very low levels at ICRs that are methylated in these male germ cells (*H19*, *Gtl2* and *Rasgrf1*). Furthermore, in somatic cells, we had found that H3K4me2 was consistently associated with the unmethylated allele of all the ICRs analysed. This modification could therefore be linked to keeping the ICR unmethylated. We wished to explore such a possible link in male germ cells that had not yet undergone meiosis and which were still actively dividing. For this, we purified type-A spermatogonia from males at 6–7 days after birth, by using an antiserum directed against integrin alpha-6, a surface marker specifically expressed in spermatogonia (Shinohara *et al*, 1999) (see Materials and methods). Five hundred thousand spermatogonia were used for native ChIP against H3K4me2 (Figure 6). Highest levels of precipitation were obtained at the unmethylated *Igf2r* and KvDMR1 ICRs, and at the *Hprt1* CpG island, which was similar to what was observed in postmeiotic cells. At the

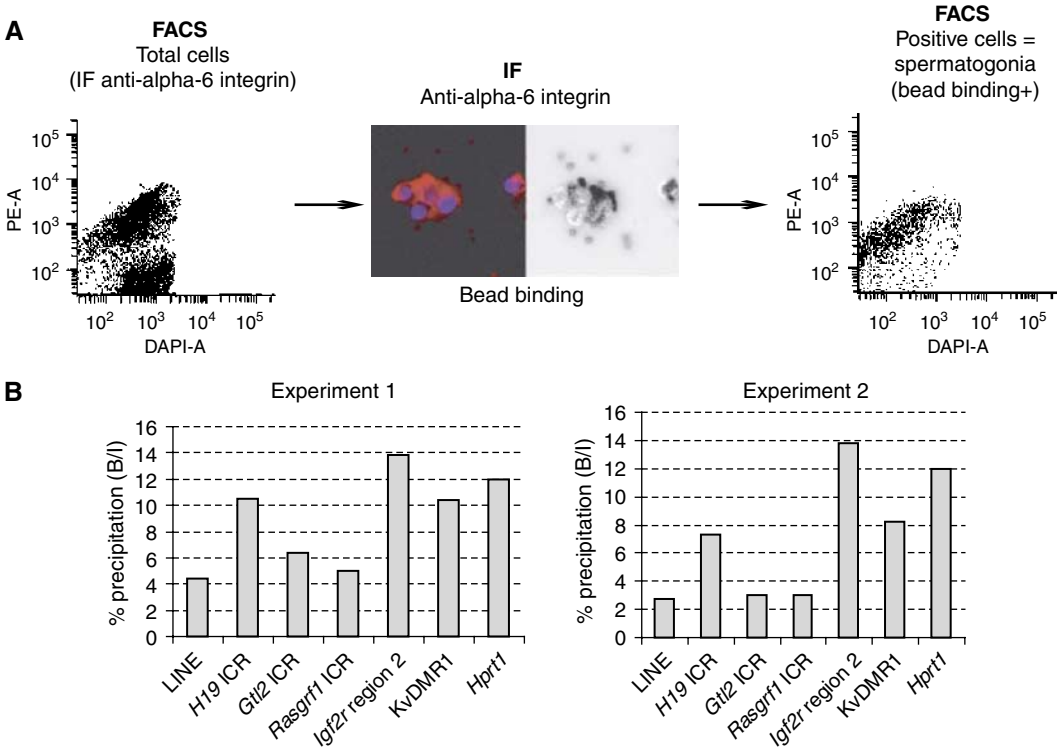

Figure 6 Analysis of H3 K4 methylation in spermatogonia. (**A**) Purification of type-A spermatogonia from 6 to 7-day-old males. Shown are cells immunostained for integrin alpha-6, purified with magnetic beads. Positively staining cells (bead binding +) are spermatogonia (Shinohara *et al*, 1999) also visualised by FACS analysis of the sorted fraction. (**B**) Five hundred thousand spermatogonia were used for ChIP against H3K4me2. Experiments were performed on two independent spermatogonial purifications. Precipitation is shown as the percentage of input chromatin brought down at the locus of interest.

DNA-methylated *Gtl2* and *Rasgrf1* ICRs (Li *et al*, 2004), and at LINE1, several-fold lower precipitation levels were obtained. An intermediate level of precipitation was observed at the *H19* ICR, which, at this early stage, still undergoes acquisition of DNA methylation (Davis *et al*, 2000; Ueda *et al*, 2000).

Discussion

One conclusion from this study is that in somatic cells, ICRs with paternal DNA methylation are marked by allele-specific H3 and H4 modifications, similar to ICRs with maternal DNA methylation. This suggests a putative role for these histone modifications in the maintenance of allelic DNA methylation at ICRs. The three ICRs with paternal methylation are exceptional, however, in that their sperm-derived DNA methylation is protected against the global wave of demethylation that occurs after fertilisation. We explored whether this could be linked to events during spermatogenesis, and found that the paternally and maternally methylated ICRs are marked by different combinations of histone modifications during the spermatogenic stages preceding the genome-wide histone-to-protamine exchange. We hypothesise that these pronounced differences could impact on how chromatin at these regions is assembled into specific structures during the final stages of spermiogenesis, and may thus determine in which configuration ICRs are transmitted to the fertilised egg.

Most germline-marked regions that control imprinting have oocyte-derived DNA methylation and correspond to promoters. ICRs with sperm-derived DNA methylation are different. They are not promoters and are not located within genes. Nevertheless, these regions are CpG-rich and their allelic methylation needs to be maintained throughout development. By ChIP, we detected pronounced allelic chromatin differences at the *H19*, *Gtl2* and *Rasgrf1* ICRs in ES and adult cells. Chromatin on the DNA-methylated allele is consistently associated with H4-K20 and H3-K9 trimethylation, but not with H3K27me3. In contrast, chromatin on the allele without DNA methylation is consistently marked by H3-K4 dimethylation and H3 acetylation, despite the fact that these ICRs do not correspond to promoters. This is particularly interesting as H3-K4 methylation is a modification usually restricted to promoter regions (Bernstein *et al*, 2006). The allelic histone modifications at the *H19*, *Gtl2* and *Rasgrf1* ICRs were similar to those observed at the KvDMR1 (Figures 2 and 3) and at several other ICRs with maternal DNA methylation (unpublished data; Gregory *et al*, 2001; Fournier *et al*, 2002; Yang *et al*, 2003; Umlauf *et al*, 2004a), except for H3K27me3. In this study and in previous work (Umlauf *et al*, 2004b), we also achieved allelic enrichment of H3-K9 dimethylation, albeit less pronouncedly than that of H3-K9 trimethylation. However, little H3-K9 dimethylation was brought down at the different ICRs analysed (Supplementary Figure 1).

It is not known how trimethylation at H3-K9 and H4-K20 is linked to the somatic maintenance of DNA methylation at ICRs. There are striking similarities, however, with the organisation of pericentric heterochromatin. Also the condensed chromatin associated with pericentric satellite repeats is characterised by H3-K9 and H4-K20 trimethylation, and by DNA methylation, and is maintained in all the somatic lineages (Lehnertz *et al*, 2003; Kourmouli *et al*, 2004;

Martens *et al*, 2005). The histone methyltransferases (HMTs) Suv39h1/2 are essential for the H3-K9 trimethylation at constitutive heterochromatin, whereas the Suv4-20h HMTs are involved in regulating its H4-K20 trimethylation (Lehnertz *et al*, 2003; Kourmouli *et al*, 2004; Schotta *et al*, 2004). Whether the same, or yet-other, HMTs control trimethylation on H3-K9 and H4-K20 at mammalian ICRs is unknown. Suv39h1/2 are important for the recruitment of the DNA methyltransferase *Dnmt3b* to pericentric heterochromatin (Lehnertz *et al*, 2003), suggesting a possible link between maintenance of histone and DNA methylation (Fuks, 2005). The novel parallels between ICRs and pericentric heterochromatin also raise the question of whether they could have a similar nuclear localisation as well. In particular, in the mammalian nucleus, virtually all the H3K9me3 and H4K20me3 are located at pericentric heterochromatin, and Western analysis indicates that these trimethylation marks are largely present within the same nucleosomes (Kourmouli *et al*, 2004; Sims *et al*, 2006).

Conversely, what protects the unmethylated copy of ICRs against acquisition of DNA methylation? At ICRs with maternal DNA methylation, this could be linked to gene activity. Such a mechanism seems unlikely for the *H19*, *Gtl2* and *Rasgrf1* ICRs, as these regions do not correspond to promoters. Rather, a consistent feature of chromatin on the unmethylated allele of all the ICRs analysed was the presence of H3-K4 dimethylation, together with H3-K9 and K14 acetylation (but not H4 acetylation). *In vitro*, H3-K4 methylation prevents binding of the NURD histone deacetylase complex and could thus prevent loss of histone acetylation (Zhang *et al*, 1999; Zegerman *et al*, 2002). As HDAC1/2 associate with Dnmt1, such a mechanism could also potentially prevent DNA methylation (Fuks, 2005). Interestingly, a recent gene targeting study on Mll suggests that at Hox genes, this SET domain protein is important for maintaining H3-K4 methylation, and also for preventing DNA methylation (Terranova *et al*, 2006).

In male germ cells, at the different spermatogenic stages analysed, the *Igf2r* and KvDMR1 ICRs had high levels of H3 K4 methylation and H3 acetylation, and the same was observed for the *Hprt* CpG island. As in somatic cells, these modifications were enriched at regions without DNA methylation. Possibly also in spermatogenic cells, H3K4me2 and H3ac could be involved in preventing the chromatin from becoming DNA-methylated. For H3K4me2, we found this link in pre-meiotic spermatogonia as well, at a developmental stage where cells are still dividing. However, cell numbers are limited at premeiotic stages and more extensive chromatin studies would require novel ChIP technologies adapted for studying small cell numbers (O'Neill *et al*, 2006).

Unlike in somatic cells, in spermatocytes, round spermatids and elongating spermatids, we did not detect any enrichment of H4-K20 and H3-K9 trimethylation at the *H19*, *Gtl2* and *Rasgrf1* ICRs, despite the fact that these regions had high levels of DNA methylation. At these meiotic and postmeiotic stages, therefore, these histone methylation marks are not associated with the presence of DNA methylation, but cells do no longer proliferate either.

An important conclusion from this first locus-specific analysis of spermatogenesis is that different ICRs are marked by different combinations of histone modifications. Whereas H3-K4 methylation and H3 acetylation are strongly enriched at ICRs with maternal DNA methylation (*Igf2r* region 2 and the KvDMR1), these modifications are absent on the chromatin at the three paternal ICRs. H4 acetylation, in contrast, is detected at all the regions analysed. A challenge for the future will be to explore the significance of these different combinations of histone modifications. For instance, is the presence of H4 acetylation on its own sufficient to allow for subsequent histone-to-protamine exchange, possibly involving the testis-specific bromodomain protein BRDT (Hazzouri *et al*, 2000; Pivot-Pajot *et al*, 2003)? Or, rather, would certain combinations of modifications on H4 and other histones provide the signal for this chromatin remodelling during spermiogenesis? Particularly, does the absence of H3-K4 methylation and H3 acetylation (but presence of H4 acetylation) at the *H19*, *Gtl2* and *Rasgrf1* ICRs still allow histone-to-protamine exchange during late spermiogenesis? If not, in which chromatin configuration are these regions transmitted by the sperm to the fertilised egg? Interestingly, we detected high levels of H4-K20 methylation at LINE1 sequences, and chromatin at these repeats was also enriched in H4 acetylation. This combination of H4 modifications was not observed in any of the other regions, suggesting that it could be specific to LINE1 (and possibly other) repeats and could signal the formation of specific structures later in spermatogenesis.

The combinations of histone modifications present at the different analysed loci raise the question whether testis-specific histone variants could be selectively recruited to form specific structures during late spermatogenesis. This has been suggested for the recently identified H1 variant H1T2, which accumulates at the acrosomal side of the nucleus during late spermatogenesis (Martianov *et al*, 2005). Additionally, in certain chromatin contexts, non-histone proteins could bind to methylated DNA sequences and could thus affect their subsequent recognition and remodelling. Present chromatin technologies are not well adapted to address these questions in a locus-specific manner during and after the global histone-to-protamine exhange (i.e., in condensed spermatids and mature sperm). However, based on immunostaining against H4K20me3, it has been suggested that a small percentage of the genomic DNA remains packaged with histones in mature mouse sperm (Kourmouli *et al*, 2004). In human sperm, up to 15% of genomic DNA could be associated with histones rather than protamines (Gatewood *et al*, 1987; Gardiner-Garden *et al*, 1998). One possibility would be that paternal ICRs, and other regions that are protected against paternal DNA demethylation in the zygote, do not undergo the canonical histone-to-protamine exchange and remain nucleosomally organised in mature sperm. The present ChIP studies on spermatocytes, round spermatids and elongating spermatids provide a first indication of this possibility.

Materials and methods

ES cells and adult tissues

Livers were dissected from mice obtained by crossing C57BL/6 females with *M. molosinus* males. Animal husbandry and breeding were licensed by the 'Direction Départementale des Services Vétérinaires'. For ChIP on ES cells (passages 19–21), line SF1-G was grown as described before (Dean *et al*, 1998). For expression studies, brain and testis were dissected from >8-week-old males.

ChIP on somatic cells and tissues, and allelic discrimination by SSCP

ChIP was performed on adult liver and on undifferentiated ES cells. Most antibodies used were purchased from Upstate Biotechnology, Lake Placid, NY: these were directed against dimethyl H3-K4 (#07-030), dimethyl H3-K9 (#07-212), trimethyl H3-K9 (#07-442), acetyl H3-K9 (#06-942), acetyl H3-K9 + 14 (#06-599), trimethyl H4-K20 (#07-463), acetyl H4 (#06-866) and H2A(#07-146). Antiserum against H3K27me3 was obtained from Dr Yi Zhang and the antiserum against TP2 was from Dr WS Kistler. The anti-H3 antibody was purchased from AbCam (#ab1791-100). Unfixed chromatin fragments of 1–7 nucleosomes in length were prepared as described before (Umlauf *et al*, 2004b). About 3 μg of chromatin was used per ChIP, using ~2 μg of affinity-purified antibody. Amplification by radio active PCR was with primers described in Supplementary Table I. Parental alleles were distinguished by electrophoretic detection of SSCPs in the PCR products (Gregory *et al*, 2001). Maternal and paternal band intensities were determined using Aida-2 software. Each experiment was performed on 2–3 independent chromatin preparations.

ChIP on spermatogenic cells

Spermatogenic cells obtained from testes of 8–10-week-old males were fractionated using the Bellvé method (Bellve, 1993), described in detail in Pivot-Pajot *et al* (2003). Briefly, mouse testes were dissected and processed to obtain a homogeneous cell suspension. Cells were then laid on top of a 2–4% BSA gradient in an airtight sedimentation chamber at 4°C. Fractions were collected after 70 min, were developmentally staged using a phase-contrast microscope and were pooled to obtain cell populations enriched in each of the stages: spermatocytes, round spermatids and a mix of elongating (70%) and round spermatids (30%). Cells were resuspended and lysed in 15 mM Tris–HCl pH 7.4, 15 mM NaCl, 60 mM KCl, 12% sucrose, 2 mM EDTA, 0.5 mM EGTA, 0.65 mM spermidine, 0.03% Triton X-100, 1 mM DTT, protease inhibitor cocktail (Roche, according to the manufacturer's instructions), 0.5 mM PMSF and 330 nM TSA. After 10 min centrifugation at 200 *g*, the nuclear pellet was washed in the same buffer omitting EDTA, EGTA and Triton, and was centrifuged for 10 min at 200 *g*. Nuclei were resuspended in 500 μl MNase buffer (Umlauf *et al*, 2004b), and approximately 1 million nuclei were digested for 3 min with 3 U of MNase at 37°C. MNase was inactivated by adding EDTA to a concentration of 40 mM and chilling on ice. Centrifugation at 18 000 *g* for 10 min allowed us to separate the S1 fraction (corresponding to small chromatin fragments) and a second fraction of larger oligonucleosomes obtained after overnight dialysis, as described (Gregory *et al*, 2001; Umlauf *et al*, 2004a). Selected S1 and S2 fractions were mixed and used for ChIP. The ChIP procedure, washing conditions and DNA extraction from the precipitated chromatin fractions were as for chromatin from liver and ES cells. Precipitated chromatin fractions obtained after ChIP were analysed by real-time PCR (Mx3000p, Stratagene), using the Quantitect SYBR Green PCR kit (Qiagen). Primers used for PCR amplification are described in Supplementary Table II. Each PCR was run in triplicate. The experiment was performed on 2–3 independent chromatin preparations. Results were defined as the percentage of precipitation, that is, the ratio between the average value of the bound fraction and the average value of input chromatin. For purification of spermatogonia, testes from 6–7-day-old mice were decapsulated in ice-cold PGE (1 × PBS, 0.1% glucose, 1 mM EDTA) and incubated for 15 min at 35°C in the same buffer containing 1 mg/ml collagenase (Sigma) and DNase I (Roche). After a first wash in PGE (10 min at 200 *g*), cells were mechanically dissociated at 4°C for 5 min, filtered twice (100 μm Cup Falcons, BD Biosciences), resuspended in 15 ml PGE and washed again. Cells were resuspended in 1 ml PGE containing DNase I and incubated at RT for 1 h with 40 μl mouse anti-CD49t (integrin alpha-6) antibody (R-phycoerythrin-conjugated rat monoclonal antibody; BD Pharmigen). After two washes with PGE, cells were resuspended in 1 ml PGE. The proportion of positively staining cells was determined by immunofluorescence and FACS analysis (Figure 6A). The cell suspension was then mixed with 40 μl of protein G-coupled magnetic beads (Dynabeads) and incubated at 4°C for 20 min. After magnetic removal of unbound cells, cells attached to the beads were pelleted by centrifugation at 200 *g* for 5 min at 4°C. The proportion of integrin alpha-6-positive cells in the bead-bound cell fraction, assessed by IF and FACS analysis, was higher than 95%. Nuclei purification and chromatin preparation were as for the spematocytes and spermatids.

Western blotting

After fractionation, cells were disrupted in 8 mM urea and crude extracts were quantified using Bradford (Biorad Protein Assay). Western blotting of total protein extracts was performed according to the standard procedures. Antisera were used at the following dilutions: 1/1000 for H2A and TP2 and 1/2000 for the other antisera.

RNA expression and EST search

Currently available EST databases were searched by performing a BLAST search with sequences of about 2 kb in length selected so as to encompass the ICR element. Total RNA was extracted from cells and tissues using Trizol reagent (InVitrogen). cDNA was generated with the Stratascript kit (Stratagene), using random primers. cDNA samples were analysed by real-time PCR using primer pairs described in Supplementary Table I.

Supplementary data

Supplementary data are available at *The EMBO Journal* Online (http://www.embojournal.org).

Acknowledgements

We thank members of the Imprinting and Development group, and Thierry Forné, for helpful discussion and comments, Yi Zhang for the H3K27me3 antiserum and S Kistler (University of South Carolina, Columbia, USA) for the TP2 antiserum. RF acknowledges grant funding from the ESF EUROCORES programme EuroSTELLS, the CNRS, the ARC programme ARECA, the Cancéropôle Grand Sud-Ouest and the ACI programme of the French Ministry of Education and Science. SK acknowledges grant funding from CLARA Cancéropôle 'EpiMed' and 'Epipro' programmes, from ARECA (ARC) and the 'Regulome' network (ANR).

References

Bellve AR (1993) Purification, culture, and fractionation of spermatogenic cells. *Methods Enzymol* **225:** 84–113

Bernstein BE, Mikkelsen TS, Xie X, Kamal M, Huebert DJ, Cuff J, Fry B, Meissner A, Wernig M, Jaenisch R, Wagschal A, Feil R, Schreiber SL, Lander ES (2006) A bivalent chromatin structure marks key developmental genes in embryonic stem cells. *Cell* **125:** 315–326

Bourc'his D, Xu GL, Lin CS, Bollman B, Bestor TH (2001) Dnmt3L and the establishment of maternal genomic imprints. *Science* **294:** 2536–2539

Davis TL, Yang GJ, McCarrey JR, Bartolomei MS (2000) The *H19* methylation imprint is erased and re-established differentially on the parental alleles during male germ cell development. *Hum Mol Genet* **9:** 2885–2894

Dean W, Bowden L, Aitchison A, Klose J, Moore T, Meneses JJ, Reik W, Feil R (1998) Altered imprinted gene methylation and expression in completely ES cell-derived mouse fetuses: association with aberrant phenotypes. *Development* **125:** 2273–2282

Delaval K, Feil R (2004) Epigenetic regulation of mammalian genomic imprinting. *Curr Opin Genet Dev* **14:** 188–195

Ferguson-Smith AC, Surani MA (2001) Imprinting and the epigenetic asymmetry between parental genomes. *Science* **293:** 1086–1089

Fitzpatrick GV, Soloway PD, Higgins M (2002) Regional loss of imprinting and growth deficiency in mice with a targeted deletion of *KvDMR1*. *Nat Genet* **32:** 426–431

Fournier C, Goto Y, Ballestar E, Delaval K, Hever AM, Esteller M, Feil R (2002) Allele-specific histone lysine methylation marks regulatory regions at imprinted mouse genes. *EMBO J* **21:** 6560–6570

Fuks F (2005) DNA methylation and histone modifications: teaming up to silence genes. *Curr Opin Genet Dev* **15:** 490–495

Gardiner-Garden M, Ballesteros M, Gordon M, Tam PPL (1998) Histone- and protamine-DNA association: conservation of different patterns within the B-globin domain in human sperm. *Mol Cell Biol* **18:** 3350–3356

Gatewood JM, Cook GR, Balhorn R, Bradbury EM, Schmid CW (1987) Sequence-specific packaging of DNA in human sperm chromatin. *Science* **236:** 962–964

Govin J, Caron C, Lestrat C, Rousseaux S, Khochbin S (2004) The role of histones in chromatin remodelling during mammalian spermiogenesis. *Eur J Biochem* **271:** 3459–3469

Gregory RI, Randall TE, Johnson CA, Khosla S, Hatada I, O'Neill LP, Turner BM, Feil R (2001) DNA methylation is linked to deacetylation of histone H3, but not H4, on the imprinted genes *Snrpn* and *U2af1-rs1*. *Mol Cell Biol* **21:** 5426–5436

Hazzouri M, Pivot-Pajot C, Faure AK, Usson Y, Pelletier R, Sele B, Khochbin S, Rousseaux S (2000) Regulated hyperacetylation of core histones during mouse spermatogenesis: involvement of histone deacetylases. *Eur J Cell Biol* **79:** 950–960

Kaneda M, Okano M, Hata K, Sado T, Tsujimoto N, Li E, Sasaki H (2004) Essential role for *de novo* DNA methyltransferase Dnmt3a in paternal and maternal imprinting. *Nature* **429:** 900–903

Kimmins S, Sassone-Corsi P (2005) Chromatin remodelling and epigenetic features of germ cells. *Nature* **434:** 583–589

Kobayashi H, Suda C, Abe T, Kohara Y, Ikemuura T, Sasaki H (2006) Bisulphite sequencing and dinucleotide content analysis of 15 imprinted mouse differentially methylaed regions (DMRs): paternally methylated DMRs contain less CpGs than maternally methylated DMRs. *Cytogenet Genome Res* **113:** 130–137

Kourmouli N, Jeppesen P, Mahadevhaieh S, Burgoyne P, Wu R, Gilbert DM, Bongiorni S, Prantera G, Fanti L, Pimpinelli S, Shi W, Fundele R, Singh PB (2004) Heterochromatin and trimethylated lysine 20 of histone H4 in animals. *J Cell Sci* **117:** 2491–2501

Lehnertz B, Ueda Y, Derijck AA, Brainschweig U, Perez-Burgos L, Kubicek S, Cen T, Li E, Jenuwein T, Peters AH (2003) Suv39h-mediated histone H3 lysine 9 methylation directs DNA methylation to major satellite repeats at pericentric heterochromatin. *Curr Biol* **13:** 1192–1200

Li E, Beard C, Jaenisch R (1993) Role of DNA methylation in genomic imprinting. *Nature* **366:** 362–365

Li JY, Lees-Murdock DJ, Xu GL, Walsh CP (2004) Timing of establishment of paternal methylation imprints in the mouse. *Genomics* **84:** 952–960

Lin SP, Youngson N, Takada S, Seitz H, Reik W, Paulsen M, Cavaillé J, Ferguson-Smith AC (2003) Asymmetric regulation of imprinting on the maternal and paternal chromosomes at the *Dlk1-Gtl2* imprinted cluster on mouse chromosome 12. *Nat Genet* **35:** 97–102

Mancini-Dinardo D, Steele SJ, Levorse JM, Ingram JM, Tilghman SM (2006) Elongation f the Kcnq1ot1 transcript is required for genomic imprinting of neighboring genes. *Genes Dev* **20:** 1268–1282

Martens JH, O'Sullivan RJ, Braunschweig U, Opravil S, Radolf M, Steinlein P, Jenuwein T (2005) The profile of repeat-associated histone lysine methylation sates in the mouse epigenome. *EMBO J* **24:** 800–812

Martianov I, Brancorsini S, Catena R, Gansmuller A, Kotaja N, Parvienene M, Sassone-Corsi P, Davidson I (2005) Polar nuclear localization of H1T2, a histone H1 variant, required for spermatid elongation and DNA condensation during spermiogenesis. *Proc Natl Acad Sci USA* **102:** 2808–2813

Mayer W, Niveleau A, Walter J, Fundele R, Haaf T (2000) Demethylation of the zygotic paternal genome. *Nature* **403:** 501–502

Meistrich ML, Mohapatra B, Shirley CR, Zhao M (2003) Roles of transition nuclear proteins in spermiogenesis. *Chromosoma* **111:** 483–488

Namekawa S, Park PJ, Zhang L-F, Shima JE, McCarrey JR, Griswold MD, Lee JT (2006) Postmeiotic sex chromatin in the male germ line of mice. *Curr Biol* **16:** 660–667

O'Neill LP, VerMilea MD, Turner BM (2006) Epigenetic characterization of the early embryo with a chromatin immunoprecipitation protocol applicable to small cell populations. *Nat Genet* **38:** 835–841

Oswald J, Engemann S, Lane N, Mayer W, Olek A, Fundele R, Dean W, Reik W (2000) Active demethylation of the paternal genome in the mouse zygote. *Curr Biol* **10:** 475–478

Peters AHFM, Kubicek S, Mechter K, O'Sullivan RJ, Derijck AAHA, Perez-Burgos L, Kohlmaier A, Opravil S, Tachibana M, Shinkai Y, Maxtens JH, Jenuwein T (2003) Partitioning and plasticity of repressive histone methylation states in mammalian chromatin. *Mol Cell* **12:** 1577–1589

Pivot-Pajot C, Caron C, Govin J, Vion A, Rousseaux S, Khochbin S (2003) Acetylation-dependent chromatin reorganisation by BRDT, a testis-specific bromodomain-containing protein. *Mol Cell Biol* **23:** 5354–5365

Reik W, Walter J (2001) Genomic imprinting: parental influence on the genome. *Nat Rev Genet* **2:** 21–32

Schotta G, Lachner M, Sarma K, Ebert A, Sengupta R, Reuter G, Reinberg D, Jenuwein T (2004) A silencing pathway to induce H3-K9 and H4-K20 trimethylation at constitutive heterochromatin. *Genes Dev* **18:** 1251–1262

Seidl CI, Stricker SH, Barlow DP (2006) The imprinted Air ncRNA is an atypical RNAPII transcript that evades splicing and escapes nuclear transport. *EMBO J* **25:** 3565–3575

Shinohara T, Avarbock MR, Brinster RL (1999) Beta 1- and alpha 6 integrin are surface markers on mouse spermatogonial stem cells. *Proc Natl Acad Sci USA* **96:** 5504–5509

Sims JK, Houston SI, Magazinnik T, Rice JC (2006) A trans-tail histone code defined by monomethylated H4 Lys-20 and H3 Lys-9 demarcates distinct regions of silent chromatin. *J Biol Chem* **281:** 12760–12766

Takada S, Paulsen M, Teverdale M, Tsai CE, Kelsey G, Cattanach BM, Ferguson-Smith AC (2002) Epigenetic analysis of the *Dlk1-Gtl2* imprinted domain on mouse chromosome 12: implications for imprinting control from comparison with *Igf2-H19*. *Hum Mol Genet* **11:** 77–86

Terranova R, Agherbi H, Boned A, Meresse S, Djabali M (2006) Histone and DNA methylation defects at Hox genes in mice expressing a SET domain-truncated form of Mll. *Proc Natl Acad Sci USA* **103:** 6629–6634

Thorvaldsen JL, Duran KL, Bartolomei MS (1998) Deletion of the *H19* differentially methylated domain results in loss of imprinted expression of *H19* and *Igf2*. *Genes Dev* **12:** 3693–3702

Ueda T, Abe K, Miura A, yuzuriha M, Zubair M, Noguchi M, Niwa K, Kawase Y, Kono T, Matsuda Y, Fujimoto H, Shibata H, Hayashizaki Y, Sasaki H (2000) The paternal methylation imprint of the mouse *H19* gene locus is acquired in the gonocyte stage during foetal testis development. *Genes Cells* **5:** 649–659

Umlauf D, Goto Y, Feil R (2004a) Site specific analysis of histone acetylation and methylation. *Methods Mol Biol* **287:** 99–120

Umlauf D, Goto Y, Cao R, Cerqueira F, Wagschal A, Zhang Y, Feil R (2004b) Imprinting along the *Kcnq1* domain on mouse chromosome 7 involves repressive histone methylation and recruitment of Polycomb group complexes. *Nat Genet* **36:** 1296–1300

Wutz A, Smrzka OW, Schweifer N, Schellander K, Wagner EF, Barlow DP (1997) Imprinted expression of the *Igf2r* gene depends on an intronic CpG island. *Nature* **389:** 745–749

Yang Y, Li T, Vu TH, Ulaner GA, Hu JF, Hoffman AR (2003) The histone code regulating expression of the imprinted mouse *Igf2r* gene. *Endocrinology* **144:** 5658–5670

Yoon BJ, Herman H, Sikora A, Smith LT, Plass C, Soloway PD (2002) Regulation of DNA methylation of *Rasgrf1*. *Nat Genet* **30:** 92–96

Zegerman P, Canas B, Pappin D, Kouzarides T (2002) Histone H3 lysine-4 methylation disrupts binding of nucleosome remodelling and deacetylase (NuRD) repressor complex. *J Biol Chem* **277:** 11621–11624

Zhang Y, Ng HH, Erdjument-Bromage H, Tempst P, Bird A, Reinberg D (1999) Analysis of the NuRD subunits reveals a histone deacetylase core complex and a connection with DNA methylation. *Genes Dev* **13:** 1924–1935